

Effects of phosphorus doping on the physical properties ofaxion insulator candidate $EuIn_2As_2$

Feihao Pan(潘斐豪), Congkuan Tian(田丛宽), Jiale Huang(黄嘉乐), Daye Xu(徐大业), Jinchen Wang (汪晋辰), Peng Cheng(程鹏)[†], Juanjuan Liu(刘娟娟)[‡], and Hongxia Zhang(张红霞)[§]

Citation: Chin. Phys. B, 2022, 31 (**5**): 057502. DOI: 10.1088/1674-1056/ac5d2c
Journal homepage: http://cpb.iphy.ac.cn; http://iopscience.iop.org/cpb

What follows is a list of articles you may be interested in

Progress of novel diluted ferromagnetic semiconductors with decoupled spin and charge doping: Counterparts of Fe-based superconductors

Shengli Guo(郭胜利), Fanlong Ning(宁凡龙)
Chin. Phys. B, 2018, 27 (**9**): 097502. DOI: 10.1088/1674-1056/27/9/097502

Size-dependent exchange bias in single phase Mn_3O_4 nanoparticles

Song-Wei Wang(王松伟), Xin Zhang(张鑫), Rong Yao(姚蓉), Guang-Hui Rao(饶光辉)
Chin. Phys. B, 2016, 25 (**11**): 117502. DOI: 10.1088/1674-1056/25/11/117502

Spin-cluster glass state in $U(Ga_{0.95}Mn_{0.05})_3$

Dong-Hua Xie(谢东华), Wen Zhang(张文), Yi Liu(刘毅), Wei Feng(冯卫), Yun Zhang(张云), Shi-Yong Tan(谭世勇), Xie-Gang Zhu(朱燮刚), Qiu-Yun Chen(陈秋云), Qin Liu(刘琴), Bing-Kai Yuan(袁秉凯), Xin-Chun Lai(赖新春)
Chin. Phys. B, 2016, 25 (**4**): 047502. DOI: 10.1088/1674-1056/25/4/047502

Asymmetric exchange bias training effect in spin glass (FeAu)/FeNi bilayers

Rui Wen-Bin, He Mao-Cheng, You Biao, Shi Zhong, Zhou Shi-Ming, Xiao Ming-Wen, Gao Yuan, Zhang Wei, Sun Li, Du Jun
Chin. Phys. B, 2014, 23 (**10**): 107502. DOI: 10.1088/1674-1056/23/10/107502

The spin dynamics of the random transverse Ising chain with a double-Gaussian disorder

Liu Zhong-Qiang, Jiang Su-Rong, Kong Xiang-Mu
Chin. Phys. B, 2014, 23 (**8**): 087505. DOI: 10.1088/1674-1056/23/8/087505

Effects of phosphorus doping on the physical properties of axion insulator candidate $EuIn_2As_2$

Feihao Pan(潘斐豪), Congkuan Tian(田丛宽), Jiale Huang(黄嘉乐), Daye Xu(徐大业), Jinchen Wang (汪晋辰), Peng Cheng(程鹏)[†], Juanjuan Liu(刘娟娟)[‡], and Hongxia Zhang(张红霞)[§]

Laboratory for Neutron Scattering and Beijing Key Laboratory of Optoelectronic Functional Materials and MicroNano Devices, Department of Physics, Renmin University of China, Beijing 100872, *China*

(Received 24 January 2022; revised manuscript received 25 February 2022; accepted manuscript online 14 March 2022)

We report an investigation on the single crystal growth, magnetic and transport properties of $EuIn_2(As_{1-x}P_x)_2$ ($0 \leq x \leq 1$). The physical properties of axion insulator candidate $EuIn_2As_2$ can be effectively tuned by P-doping. With increasing x, the c-axis lattice parameter decreases linearly, the magnetic transition temperature gradually increases and ferromagnetic interactions are enhanced. This is similar to the previously reported high pressure effect on $EuIn_2As_2$. For $x = 0.40$, a spin glass state at $T_g = 10$ K emerges together with the observations of a butter-fly shaped magnetic hysteresis and slow magnetic behavior. Besides, magnetic transition has great influence on the charge carriers in this system and negative colossal magnetoresistance is observed for all P-doped samples. Our findings suggest that $EuIn_2(As_{1-x}P_x)_2$ is a promising material playground for exploring novel topological states.

Keywords: axion topological insulator

PACS: 75.50.Lk, 72.25.Rb,03.65.Vf **DOI:** 10.1088/1674-1056/ac5d2c

1. Introduction

Topological materials with intrinsic magnetic order may host novel quantum states such as axion topological insulator (ATI) state with topological magnetoelectric effect.[1–3] Therefore extensive efforts have been devoted in search for such materials both theoretically and experimentally.[4–11] Current researches are limited to very few classes of materials, such as the Mn–Bi–Te layered compounds.[12–19] Although many exotic magnetic and electronic states with various topological phase transitions were reported, the experimental realization of ATI phase is still controversial.[20–24]

Recently, two-dimensional layered material $EuIn_2As_2$ was theoretically proposed to be a candidate material of axion insulator with antiferromagnetic (AFM) long-range order.[5] Interestingly, the nontrivial topological state is closely related to its the magnetic ordering state. First-principles calculations show that $EuIn_2As_2$ is a topological crystalline insulator if the moments of Eu lie in the a- or b-axis and a high-order topological insulator if the moments are along c-axis. They can all host ATI states.[5] Experimentally, the orientation of the magnetic moment for the ground state of $EuIn_2As_2$ is determined to be within the ab-plane through magnetic and transport measurements.[25] Angle-resolved photoemission spectroscopy (ARPES) revealed a band reconstruction associated with the antiferromagnetic (AFM) transition together with a signature of bulk-band inversion in the AFM phase, consistent with the band calculation that supports the axion insulator phase.[26,27] Moreover, a neutron scattering investigation reveals a complex helical antiferromagnetic order in $EuIn_2As_2$ different from the collinear AFM order predicted before.[28] Since different magnetic structure may induce different topological states, it would be important for exploring the ways to tune the magnetic order in $EuIn_2As_2$. Chemical doping has been proved to be an effective method to tune the physical properties of magnetic materials.[29,30] A very recent experimental work showed that, in Ca-doped $EuIn_2As_2$, the carrier density of electrons is significantly enhanced and while the intrinsic magnetic order in this system is maintained.[31] This work also mentioned an unsuccessful try to dope phosphorus (P) into $EuIn_2As_2$.[31] In this paper, we report the successful doping of P into $EuIn_2As_2$. High-quality single crystals of $EuIn_2(As_{1-x}P_x)_2$ can be obtained from $x = 0$ to $x = 1$ and the c-axis lattice parameter continuously decreases. The magnetic properties and the magnetoresistance can be effectively tuned by P-doping and a spin-glass state is found for $x = 0.40$. Our results indicate that $EuIn_2(As_{1-x}P_x)_2$ can serve as a new material playground for further investigations and provide useful information for realizing the nontrivial topological state in this system.

2. Experimental methods

The single crystals of $EuIn_2(As_{1-x}P_x)_2$ were grown by flux method similar to previous reports.[32] A molar ratio of Eu:In:As:P = $1 : 12 : 3x : 3(1-x)$ (nominal doping concentration $x = 0.00, 0.25, 0.50, 0.75, 1.00$) was used, where In in large excess serves as the flux. All reagents were handled

[†]Corresponding author. E-mail: pcheng@ruc.edu.cn
[‡]Corresponding author. E-mail: juanjuanliu@ruc.edu.cn
[§]Corresponding author. E-mail: hxzhang@ruc.edu.cn

© 2022 Chinese Physical Society and IOP Publishing Ltd

in a Ar-filled glove box. For each reaction, all elements were mixed in an alumina crucible with half the indium flux loaded on the bottom and half on top of the rest of the reactants. The crucible, sandwiched between two layers of tightly packed quartz wool, was subsequently sealed under a 1/5 atmosphere of argon in a fused silica ampule. The reaction vessel was heated at the rate of 60 °C/h to 1100 °C and maintained at this temperature for 12 h before it was slow-cooled to 700 °C at a rate of 2 °C/h in a box furnace. The ampule was removed from the furnace at 700 °C, inverted, and centrifuged to remove the molten indium flux. Black plate-like $EuIn_2(As_{1-x}P_x)_2$ crystals with typical dimensions of $2 \times 1 \times 0.1$ mm^2 could be obtained.

X-ray diffraction (XRD) patterns of single crystals were collected from a Bruker D8 Advance x-ray diffractometer using Cu K_α radiation. The elemental doping composition was measured by energy dispersive x-ray spectroscopy (EDS, Oxford X-Max 50). Magnetization measurements were carried out in Quantum Design MPMS3 and electric transport measurements were performed on PPMS-14T.

3. Results and discussion

The elemental compositions of all single crystals were measured by EDS and the results are consistent with the formation of Eu-122 phase. The doping concentration x determined by EDS deviates from the nominal one to some extent, so all the x referred to in this paper follows the EDS results. It should be noted that the EDS result also reveals a homogeneous distribution of x for these crystals and no possible phase separations could be identified. Single crystals with five typical doping concentration (x =0, 0.40, 0.63, 0.89 and 1) were selected for further measurements. Figure 1(a) shows the XRD patterns from the *ab*-plane of these single crystals. The results are consistent with previous reports on $EuIn_2As_2$ and $EuIn_2P_2$,[32,33] no impurities could be identified.

Figure 1(b) plots the *c*-lattice parameters as a function of x. The *c*-lattice parameter decreases linearly with increasing x, which is consistent with the successful doping of P into the lattice of $EuIn_2As_2$. Apparently, partial substitution of As with P generates chemical pressure to this system and results in the shrinkage of $EuIn_2As_2$ lattice along the *c*-axis.

The results of DC magnetization measurements on $EuIn_2(As_{1-x}P_x)_2$ are shown in Fig. 2. For undoped $EuIn_2As_2$, the temperature dependent magnetic susceptibility $\chi(T)$ under 1 kOe exhibits an AFM-like cusp at $T_N = 16$ K for both $H \parallel ab$ and $H \parallel c$, supporting an AFM ground state same as previous reports.[32] The isothermal magnetization $M(H)$ at 2 K shows that $EuIn_2As_2$ can be fully polarized to a ferromagnetic state with $H > 10$ kOe when the magnetic field is applied within *ab*-plane. The saturation field for $H \parallel c$ is much bigger than that needed for $H \parallel ab$, confirming that $EuIn_2As_2$ is an easy-plane magnetic material. This easy-plane magnetic anisotropy is observed for all P-doped samples as revealed from isothermal magnetization [Figs. 2(f)–2(j)]. It should be noted that demagnetization corrections have been applied on the $H \parallel c$ data and H_{int} is the internal field. The saturation moments for $EuIn_2(As_{1-x}P_x)_2$ are all close to 7.3 μ_B/Eu which is almost doping independent and consistent with the theoretical value for a free Eu^{2+}.

The magnetic properties of $EuIn_2(As_{1-x}P_x)_2$ can be effectively tuned by doping concentration x. For $x = 0.40$, the magnetic transition temperature increases to 18 K, which is determined as the temperature at which $\chi_c(T)$ has an cusp-like feature and $d\chi_{ab}/dT$ has an minimum [inset of Fig. 2(b)]. Interestingly, a bifurcation between zero-field-cooling (ZFC) and field-cooling (FC) $\chi_{ab}(T)$ curves is observed at $T_g = 10$ K which indicates the emergence of a spin-glass behavior.[34,35] With more P-doping, it can be seen that the cusp-like feature disappear in $\chi_{ab}(T)$ under $H = 1$ kOe. Nevertheless, the minimum of $d\chi_{ab}/dT$ still exists and occurs at the sample temperature with the cusp-like feature in $\chi_c(T)$ curves. Therefore the magnetic tranistion temperature T_M at higher doping level can still be determined by this method and it increases to $T_M = 24$ K for $x = 0.89$ and $x = 1$. Furthermore, the initial isothermal magnetization has a very sharp increase versus field at $T = 2$ K and $H \parallel ab$ for $x \geqslant 0.63$ compared to undoped $EuIn_2As_2$, as marked by the black arrows in Figs. 2(h)–2(j). This is an indication of enhanced ferromagnetic interactions within *ab*-plane. Recently, the increased magnetic transition temperature and the enhancement of intralayer ferromagnetic exchange coupling are also observed in $EuIn_2As_2$ by means of high pressure.[36] So the doping of P can somehow demonstrate the high pressure effect on $EuIn_2As_2$.

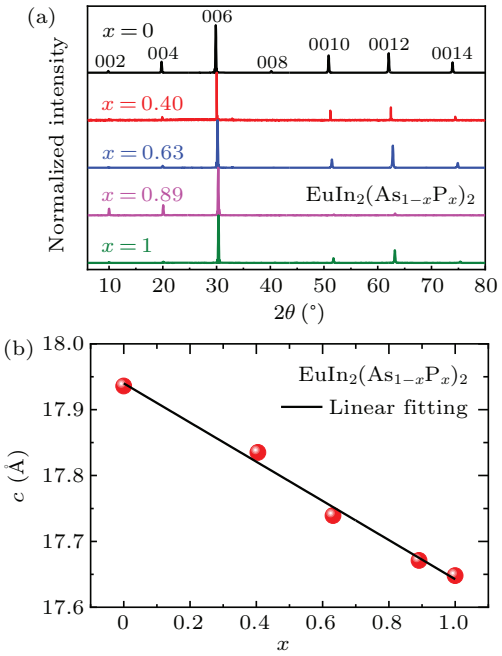


Fig. 1. (a) XRD patterns from the *ab*-plane of $EuIn_2(As_{1-x}P_x)_2$ single crystals at room temperature. (b) The doping dependent *c*-axis lattice parameters for $EuIn_2(As_{1-x}P_x)_2$.

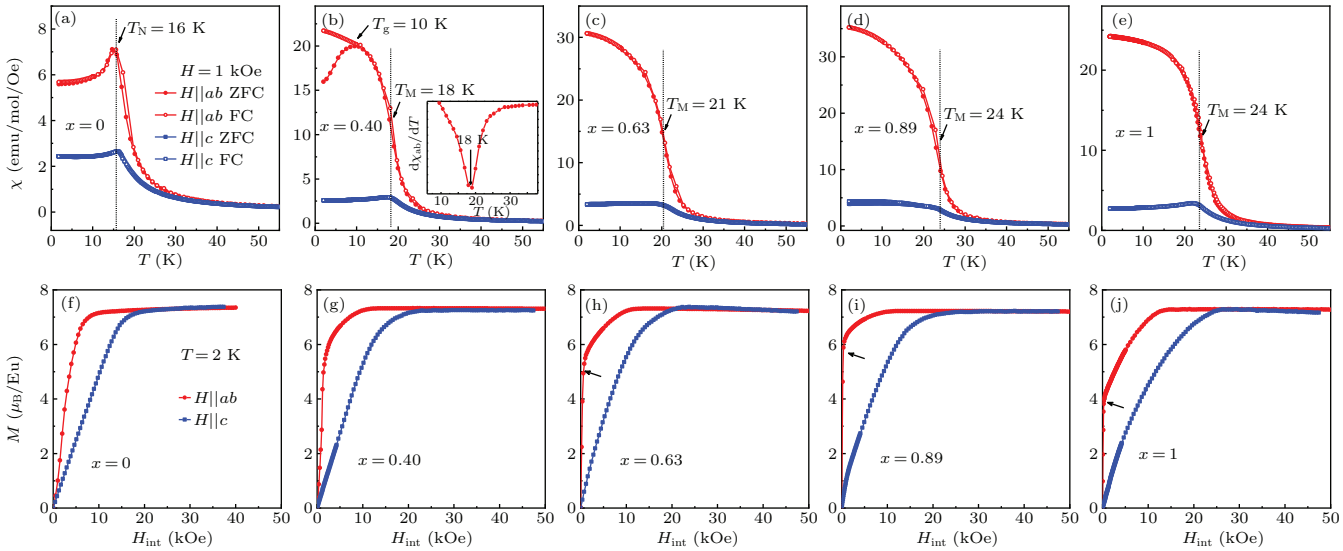


Fig. 2. Temperature dependent magnetic susceptibilities at $H = 1$ kOe [(a)–(e)] and isothermal magnetization measured at $T = 2$ K [(f)–(j)] for $EuIn_2(As_{1-x}P_x)_2$. The inset of (b) shows the $d\chi_{ab}/dT$ curve for $x = 0.40$.

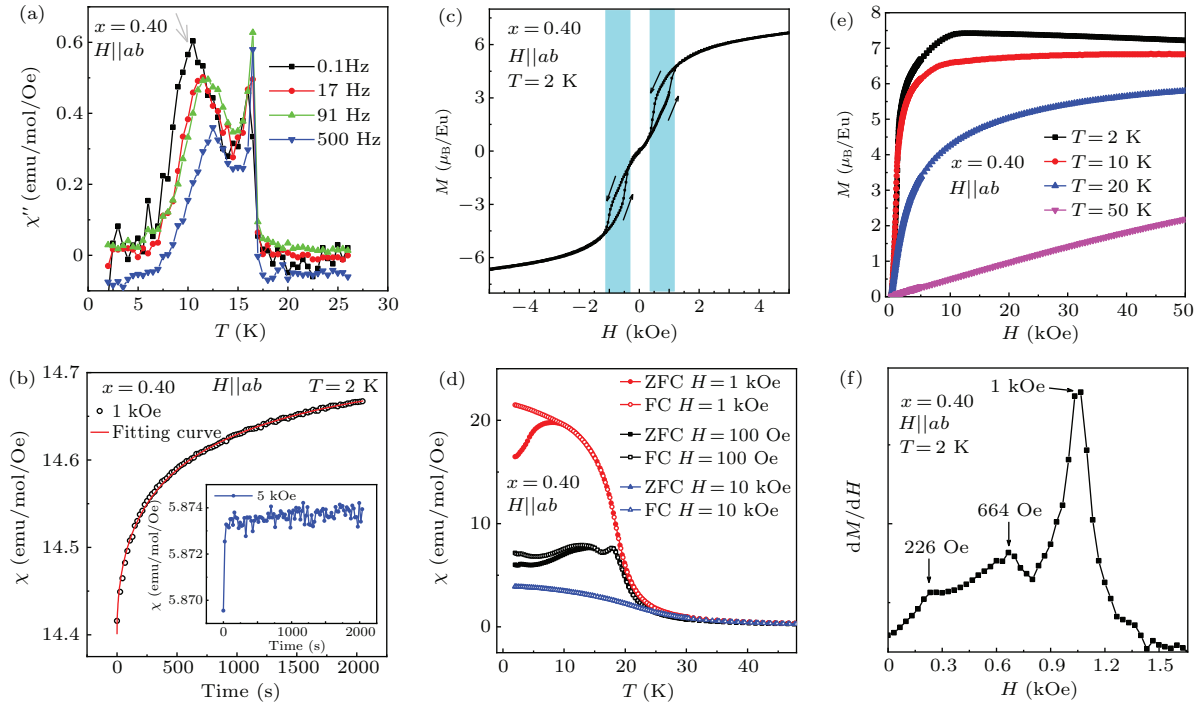


Fig. 3. Detailed magnetization data for $x = 0.40$ along $H \parallel ab$. (a) The temperature dependent imaginary part χ'' of AC susceptibility. (b) Time dependent of magnetization when the magnetic field is fast settled to 1 kOe at 2 K. The inset shows similar measurement with $H = 5$ kOe. (c) Hysteresis loop at 2 K. (d) The temperature dependent susceptibilities under different fields. (e) $M(H)$ curves at different temperatures. (f) The dM/dH as a function of field at 2 K.

In order to further verify the spin glass state of the $x = 0.40$ sample, more detailed magnetization measurements along $H \parallel ab$ were performed. Firstly, the temperature dependent imaginary part χ'' of AC susceptibility is shown in Fig. 3(a), which is measured under oscillating AC field of 5.0 Oe and a static DC field of 500 Oe. The peak near $T_g = 10$ K exhibits a clear shift towards higher temperature with increasing frequencies, which confirms the spin glass state in this sample. Secondly, the hysteresis loop of the magnetization at $T = 2$ K adopts a anomalous butterfly shape as shown in Fig. 3(c). Magnetic hysteresis is observed when the absolute value of field is between 0.3 kOe and 1.2 kOe. Within this field region, a small portion of magnetic moments ($\sim 2\%$) exhibit a significant slow magnetic relaxation. This is observed through the time dependent magnetization measurement when the sample is fast settled to 1 kOe in ZFC mode [Fig. 3(b)]. The relaxation curve $\chi(t)$ can be well fitted by a stretched exponential equation[37]

$$\chi(t) = \chi_0 - \chi_1 e^{-(\frac{t}{\tau})^{0.5}}. \quad (1)$$

The extracted relaxation time τ is 643 s. This slow magnetic

behavior and hysteresis at low-field region should be due to the spin-glass state in $x = 0.40$ sample.[34,35] With increasing magnetic field, as shown in Fig. 3(d) and the inset of Fig. 3(b), the bifurcation between ZFC and FC $\chi_{ab}(T)$ curves, the magnetic hysteresis and the slow magnetic behavior all disappear. This is consistent with a spin glass state which could be easily suppressed by field.[34]

The emergence of spin glass state in $x = 0.40$ could be explained by doping-induced disorder effect. On the other hand, the gradually enhanced in-plane ferromagnetic interactions at higher P-doping concentration is clearly shown in the magnetization measurements. This also gives a natural explanation for the spin glass state, which is due to the competition between antiferromagnetic and ferromagnetic interactions tuned by P-doping.[34] For $x = 0.40$, this competition may be enhanced at lower temperature and bring the spin glass state at T_g.

The $M(H)$ curves at different temperatures for $x = 0.40$ are presented in Fig. 3(e). The ferromagnetic-like nonlinear $M(H)$ curves could be observed up to $T = 20$ K. For $EuIn_2As_2$, previous publication identified two peaks in the dM/dH curve at $T = 2$ K and $H \parallel ab$, which is interpreted as the occurrence of the spin-flop transitions.[25] For $EuIn_2(As_{1-x}P_x)_2$ with $x = 0.40$, three peaks at relatively lower magnetic field are observed from the dM/dH curve under same measuring conditions as shown in Fig. 3(f). This suggests that there are more complex field-induced metamagentic transitions and canted AFM states in the P-doped sample.[38] Finally, the magnetic phase diagram of $EuIn_2(As_{1-x}P_x)_2$ is plotted in Fig. 4, which summarizes the evolution of magnetic properties with doping concentration x.

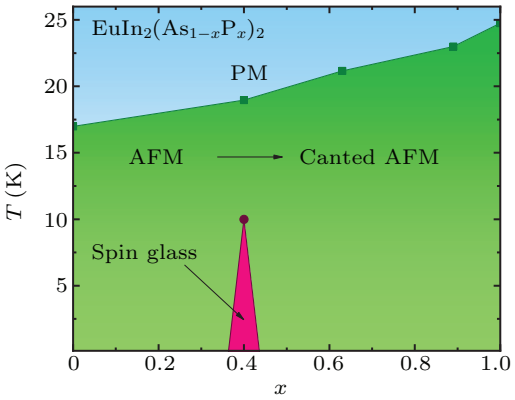


Fig. 4. Magnetic phase diagram of $EuIn_2(As_{1-x}P_x)_2$ obtained from magnetization measurements.

The electric resistances were measured for $EuIn_2(As_{1-x}P_x)_2$. As shown in Fig. 5, under zero field, all samples have a sharp cusp at around the magnetic transition temperature. This semiconductor-metal like transition feature suggests that the magnetic transition has great influences on the charge carriers in this system. Above this cusp-temperature, the short-range magnetic order may exist and the scattering induced by magnetic impurity could be enhanced with deceasing temperature, thus localize the charge carriers and induce the semiconducting-like transport properties. Below this temperature, the formation of long-range magnetic order may split the conduction band and induce the metallic resistivity.[25,32]

Both $EuIn_2As_2$ and $EuIn_2P_2$ are previously reported to exhibit negative colossal magnetoresistance. We define the magnetoresistance (MR) as $MR = [R(H) - R(0)]/R(H) \times 100\%$ and plot MR as a function of temperature in Fig. 5(b). One can see that all the P-doped samples are typical colossal magnetoresistant materials and the MR can be tuned by doping concentration x. The negative MR also has a maximum at the magnetic transition temperature for each sample. It should be noted that for $EuIn_2As_2$, at $B = 1$ T, there is positive MR region below 11 K. But for all P-doped samples, this region with positive MR disappears. The low-field positive MR in $EuIn_2As_2$ can be explained as a typical feature of AFM spin scattering.[25] Under magnetic field higher enough to polarize the AFM spins to a ferromagnetic state, the much reduced spin scattering and hopping energy give rise to a negative colossal MR. Therefore, the absence of positive MR region in P-doped samples suggest the enhancement of ferromagnetic interactions with P-doping, consistent with the magnetization data and the enhanced absolute value of negative MR at large x.

The ground state AFM structure of $EuIn_2As_2$ has been a controversial topic. Initially, it is claimed to be an collinear AFM order with ferromagnetic intralayer and antiferromagnetic interlayer couplings.[5,25] However, a more complex helical antiferromagnetic order is recently proposed in $EuIn_2As_2$ based on single-crystal neutron scattering measurements.[28] Our experimental results have shown that, for $EuIn_2(As_{1-x}P_x)_2$, the magnetic state can be effectively tuned by P-doping. Besides helical and collinear AFM order, spin glass state, canted and non-collinear AFM order may also exist in P-doped $EuIn_2As_2$. Previous density functional calculations have demonstrated that the band topology of $EuIn_2As_2$ is robust to changes of helical turn angles, magnetic order can change from A-type, to broken-helix or pure 60°-helix order while maintaining the same topological phase.[28] Therefore, further investigations could be stimulated on whether novel topological states could exist in $EuIn_2(As_{1-x}P_x)_2$. On the other hand, currently $EuIn_2As_2$ are in a metallic state with hole-type Fermi pocket.[25–27] It is important to find a way to tune the density of charge carriers and lift Fermi level, which may lead to the direct observation of the predicted topological surface state by ARPES experiment. So it would also be interesting to further investigate how P-doping could tune the chemical potential of $EuIn_2As_2$.

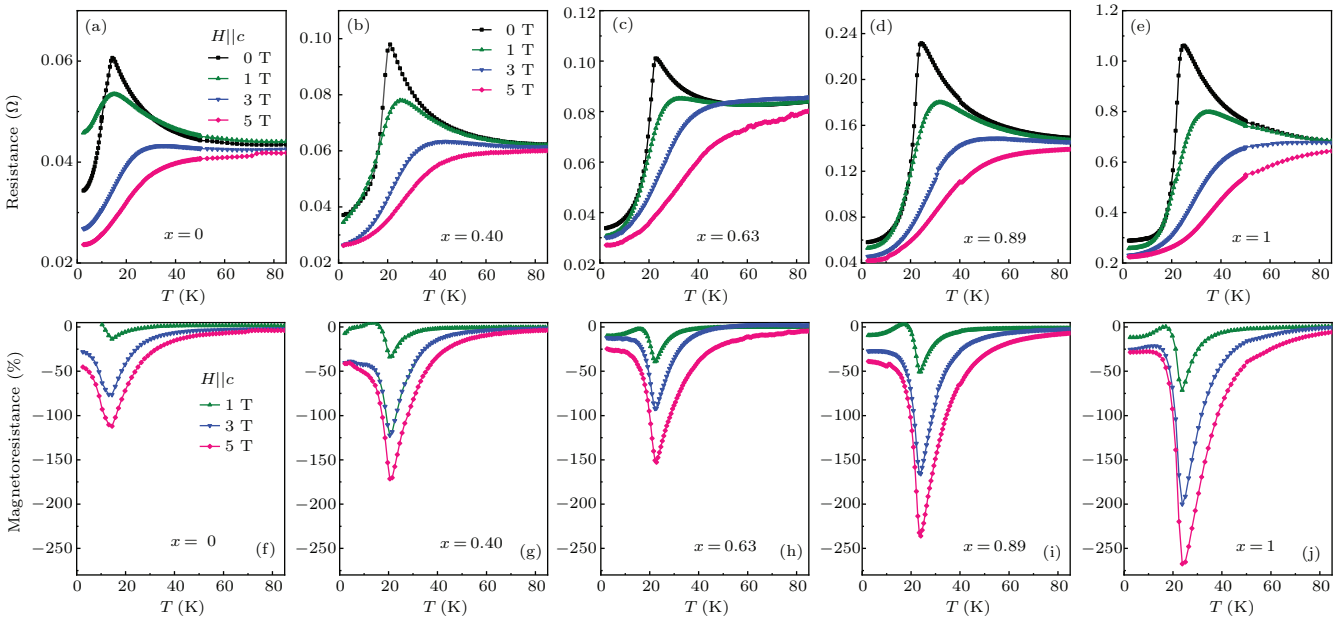


Fig. 5. (a)–(e) Temperature dependent resistances under different magnetic fields applied along $H \parallel c$ for $EuIn_2(As_{1-x}P_x)_2$. (f)–(j) The magnetoresistance defined as $[R(H)-R(0)]/R(H) \times 100\%$ of $EuIn_2(As_{1-x}P_x)_2$ is calculated and plotted.

4. Conclusion

In summary, the structural, magnetic and transport properties of $EuIn_2(As_{1-x}P_x)_2$ ($0 \leq x \leq 1$) single crystals are reported. The doping of P into the lattice of $EuIn_2As_2$ could generate chemical pressure and results in the shrinkage of $EuIn_2As_2$ lattice along the c-axis. With increasing x, the magnetization measurements reveal the enhanced ferromagnetic interaction and higher magnetic transition temperature, similar to the previously reported high pressure effect on $EuIn_2As_2$. The magnetic transition has large impact on the charge carriers and negative colossal magnetoresistance is observed in all $EuIn_2(As_{1-x}P_x)_2$ samples. Further investigations may be stimulated on whether novel topological properties may exist in $EuIn_2(As_{1-x}P_x)_2$ with variable magnetic states.

Acknowledgements

This work was supported by the National Natural Science Foundation of China (Grant Nos. 12074426, 11227906 and U2030106), the Fundamental Research Funds for the Central Universities, the Research Funds of Renmin University of China (Grant No. 20XNLG19).

References

[1] Qi X, Hughes T L and Zhang S 2008 *Phys. Rev. B* **78** 195424
[2] Essin A M, Moore J E and Vanderbilt D 2009 *Phys. Rev. Lett.* **102** 146805
[3] Li R, Wang J, Qi X and Zhang S 2010 *Nat. Phys.* **6** 284
[4] Wan X, Vishwanath A and Savrasov S Y 2012 *Phys. Rev. Lett.* **108** 146601
[5] Xu Y, Song Z, Wang Z, Weng H and Dai X 2019 *Phys. Rev. Lett.* **122** 256402
[6] Zhang D, Shi M, Zhu T, Xing D, Zhang H and Wang J 2019 *Phys. Rev. Lett.* **122** 206401
[7] Wu L, Salehi M, Koirala N, Moon J, Oh S and Armitage N P 2016 *Science* **354** 1124
[8] Dziom V, Shuvaev A, Pimenov A, Astakhov G V, Ames C, Bendias K, Böttcher J, Tkachov G, Hankiewicz E M, Brüne C, Buhmann H and Molenkamp L W 2017 *Nat. Commun.* **8** 15197
[9] Mogi M, Kawamura M, Yoshimi R, Tsukazaki A, Kozuka Y, Shirakawa N, Takahashi K S, Kawasaki M and Tokura Y 2017 *Nat. Mater.* **16** 516
[10] Li H, Gao S, Duan S, Xu Y, Zhu K, Tian S, Gao J, Fan W, Rao Z, Huang J, Li J, Yan D, Liu Z, Liu W, Huang Y, Li Y, Liu Y, Zhang G, Zhang P, Kondo T, Shin S, Lei H, Shi Y, Zhang W, Weng H, Qian T and Ding H 2019 *Phys. Rev. X* **9** 041039
[11] Chen R, Li S, Sun H, Liu Q, Zhao Y, Lu H and Xie X 2021 *Phys. Rev. B* **103** L241409
[12] Li J, Li Y, Du S, Wang Z, Gu B, Zhang S, He K, Duan W and Xu Y 2019 *Sci. Adv.* **5** eaaw5685
[13] Deng Y, Yu Y, Shi M, Guo Z, Xu Z, Wang J, Chen X and Zhang Y 2020 *Science* **367** 895
[14] Liu C, Wang Y, Li H, Wu Y, Li Y, Li J, He K, Xu Y, Zhang J and Wang Y 2020 *Nat. Mater.* **19** 522
[15] Jo N H, Wang L, Slager R J, Yan J, Wu Y, Lee K, Schrunk B, Vishwanath A and Kaminski A 2020 *Phys. Rev. B* **102** 045130
[16] Hu C, Ding L, Gordon K N, Ghosh B, Tien H J, Li H, Linn A G, Lien S W, Huang C, Mackey S, Liu J, Reddy P V S, Singh B, Agarwal A, Bansil A, Song M, Li D, Xu S, Lin H, Cao H, Chang T, Dessau D and Ni N 2020 *Sci. Adv.* **6** eaba4275
[17] Cao L, Han S, Lv Y, Wang D, Luo Y, Zhang Y, Yao S, Zhou J, Chen Y, Zhang H and Chen Y 2021 *Phys. Rev. B* **104** 054421
[18] Ji H R, Liu Y Z, Wang H, Luo J W, Li J H, Li H, Wu Y, Xu Y and Wang J 2021 *Chin. Phys. Lett.* **38** 107404
[19] Zhang J, Wang D, Shi M, Zhu T, Zhang H and Wang J 2020 *Chin. Phys. Lett.* **37** 077304
[20] Vidal R C, Bentmann H, Peixoto T R F, *et al.* 2019 *Phys. Rev. B* **100** 121104
[21] Chen Y, Xu L, Li J, Li Y, Wang H, Zhang C, Li H, Wu Y, Liang A, Chen C, Jung S, Cacho C, Mao Y, Liu S, Wang M, Guo Y, Xu Y, Liu Z, Yang L and Chen Y 2019 *Phys. Rev. X* **9** 041040
[22] Li B, Yan J, Pajerowski D M, Gordon E, Nedić A, Sizyuk Y, Ke L, Orth P P, Vaknin D and McQueeney R J 2020 *Phys. Rev. Lett.* **124** 167204
[23] Hao Y, Liu P, Feng Y, Ma X, Schwier E F, Arita M, Kumar S, Hu C, Lu R, Zeng M, Wang Y, Hao Z, Sun H, Zhang K, Mei J, Ni N, Wu L, Shimada K, Chen C, Liu Q and Liu C 2019 *Phys. Rev. X* **9** 041038
[24] Swatek P, Wu Y, Wang L, Lee K, Schrunk B, Yan J and Kaminski A 2020 *Phys. Rev. B* **101** 161109

[25] Zhang Y, Deng K, Zhang X, Wang M, Wang Y, Liu C, Mei J, Kumar S, Schwier E F, Shimada K, Chen C and Shen B 2020 *Phys. Rev. B* **101** 205126
[26] Sato T, Wang Z, Takane D, Souma S, Cui C, Li Y, Nakayama K, Kawakami T, Kubota Y, Cacho C, Kim T K, Arab A, Strocov V N, Yao Y and Takahashi T 2020 *Phys. Rev. Res.* **2** 033342
[27] Regmi S, Hosen M M, Ghosh B, Singh B, Dhakal G, Sims C, Wang B, Kabir F, Dimitri K, Liu Y, Agarwal A, Lin H, Kaczorowski D, Bansil A and Neupane M 2020 *Phys. Rev. B* **102** 165153
[28] Riberolles S X M, Trevisan T V, Kuthanazhi B, Heitmann T W, Ye F, Johnston D C, Budko S L, Ryan D H, Canfield P C, Kreyssig A, Vishwanath A, McQueeney R J, Wang L L, Orth P P and Ueland B G 2021 *Nat. Commun.* **12** 999
[29] Tian C, Wang C, Ji W, Wang J, Xia T, Wang L, Liu J, Zhang H and Cheng P 2019 *Phys. Rev. B* **99** 184428
[30] Tian C, Pan F, Xu S, Ai K, Xia T and Cheng P 2020 *Appl. Phys. Lett.* **116** 202402
[31] EnKui Y, Bin W, Han S and Bing S 2021 *Acta Phys. Sin.* **70** 127502 (in Chinese)
[32] Goforth A M, Klavins P, Fettinger J C and Kauzlarich S M 2008 *Inorg. Chem.* **47** 11048
[33] Jiang J and Kauzlarich S M 2006 *Chem. Mater.* **18** 435
[34] Binder K and Young A P 1986 *Rev. Mod. Phys.* **58** 801
[35] Li X, Sheng J, Tian C, Wang Y, Xia T, Wang L, Ye F, Tian W, Wang J, Liu J, Zhang H, Bao W and Cheng P 2018 *Europhys. Lett.* **122** 67006
[36] Yu F, Mu H, Zhuo W, Wang Z, Wang Z, Ying J and Chen X 2020 *Phys. Rev. B* **102** 180404
[37] Maignan A, Hardy V, Hébert S, Drillon M, Lees M R, Petrenko O, Paul D M K and Khomskii D 2004 *J. Mater. Chem.* **14** 1231
[38] Tian C, Pan F, Wang L, Ye D, Sheng J, Wang J, Liu J, Huang J, Zhang H, Xu D, Qin J, Hao L, Xia Y, Li H, Tong X, Wu L, Chen J H, Jia S, Cheng P, Yang J and Zheng Y 2021 *Phys. Rev. B* **104** 214410